Title
KCNKØ Opening and Closing the 2-P-Domain Potassium Leak Channel Entails “C-Type” Gating of the Outer Pore

Journal
Neuron, 32(4)

ISSN
0896-6273

Authors
Zilberberg, Noam
Ilan, Nitza
Goldstein, Steve AN

Publication Date
2001-11-01

DOI
10.1016/s0896-6273(01)00503-7

Neuron, Vol. 32, 635–648, November 20, 2001, Copyright ©2001 by Cell Press

KCNKØ: Opening and Closing the 2-P-Domain Potassium Leak Channel Entails "C-Type" Gating of the Outer Pore

Noam Zilberberg, Nitza Ilan, and Steve A.N. Goldstein[1]
Departments of Pediatrics and Cellular and Molecular Physiology
Boyer Center for Molecular Medicine
Yale University School of Medicine
New Haven, Connecticut 06536

Summary

Essential to nerve and muscle function, little is known about how potassium leak channels operate. KCNKØ opens and closes in a kinase-dependent fashion. Here, the transition is shown to correspond to changes in the outer aspect of the ion conduction pore. Voltage-gated potassium (VGK) channels open and close via an internal gate; however, they also have an outer pore gate that produces "C-type" inactivation. While KCNKØ does not inactivate, KCNKØ and VGK channels respond in like manner to outer pore blockers, potassium, mutations, and chemical modifiers. Structural relatedness is confirmed: VGK residues that come close during C-type gating predict KCNKØ sites that crosslink (after mutation to cysteine) to yield channels controlled by reduction and oxidization. We conclude that similar outer pore gates mediate KCNKØ opening and closing and VGK channel C-type inactivation despite their divergent structures and physiological roles.

Introduction

Potassium currents that develop without delay in response to voltage steps and pass current across the physiological voltage-range are called leak, background, or resting conductances (Goldman, 1943; Hodgkin et al., 1952; Hille, 1975). Such currents control excitability through their influence over resting membrane potential and, so, the duration, frequency, and amplitude of action potentials. The activity of native leak channels is strictly regulated and key to normal function of sympathetic ganglia, central neurons, and cardiac myocytes (Schmidt and Stampfli, 1966; Hille, 1973; Baker et al., 1987; Yue and Marban, 1988; Jones, 1989; Boyle and Nerbonne, 1992; Koh et al., 1992; Backx and Marban, 1993; Wu et al., 1993). The proteins mediating leak currents eluded detection, but have now been revealed to be KCNK potassium channels (Goldstein et al., 2001). More than fifty *KCNK* genes have been recognized to encode distinctive subunits with two pore-forming P loops and four predicted transmembrane segments, a 2P/4TM topology. Among sixteen recognized genes in mammals, two KCNK variants have now been recorded in cells of the central nervous system where, as expected, they influence excitability and demonstrate sensitivity to volatile anesthetics and neurotransmitters (Buckler et al., 2000; Czirjak et al., 2000; Millar et al., 2000; Sirois et al., 2000; Talley et al., 2000; Bockenhauer et al., 2001).

KCNKØ demonstrated the attributes long expected for a canonical cloned leak channel (Goldstein et al., 1996; Zilberberg et al., 2000; Ilan and Goldstein, 2001). Single channel and macroscopic KCNKØ currents change instantaneously with voltage steps to a new steady level and demonstrate open (Goldman-Hodgkin-Katz) rectification, that is, they show a linear current-voltage relationship when potassium levels are symmetrical across the membrane and outward currents under physiological conditions of high internal and low external potassium. Like classical potassium channels, KCNKØ demonstrates rapid and selective ion flux through a pathway that appears to hold multiple ions simultaneously (Ilan and Goldstein, 2001). These findings were anticipated since KCNKØ has P loop sequences similar to those that form the permeation pathways in classical potassium channels. Other studies showed that regulated changes in KCNKØ activity result from transition between a seconds-long open state and an equally lengthy closed state (C_{long}); this gating transition is kinase determined, voltage insensitive, and mediated by the cytoplasmic carboxyl terminus that determines activity by regulating the frequency of visits and duration of the long-closed state (Zilberberg et al., 2000).

Classical voltage-gated potassium (VGK) channel subunits have one P domain and six transmembrane domains (1P/6TM); they alter activity in response to changes in voltage through operation of a voltage sensor (formed by residues in the membrane-spanning segments S2 and S4) and three pore-associated gates: an activation gate located in the internal portion of the channel (Yellen, 1998; del Camino et al., 2000); an internal pore receptor for residues of the VGK subunit N terminus (or accessory β subunits) that enter and occlude the pore after it opens in a process called N-type inactivation (Hoshi et al., 1990; Zagotta et al., 1990; Demo and Yellen, 1991; Rettig et al., 1994; Zhou et al., 2001); and an external pore gate that mediates carboxy-terminal (C-type) inactivation to another nonconducting state distinguishable from the closed state (Choi et al., 1991; Hoshi et al., 1991; Liu et al., 1996; Kiss and Korn, 1998; Loots and Isacoff, 1998).

Here, we show that closing of KCNKØ involves conformational changes in the external pore that resemble C-type inactivation of VGK channels. Six lines of study support this conclusion. First, both gating steps control external pore blockade by zinc or cadmium (Yellen et al., 1994); second, both transitions are slowed by external permeant ion (Lopez et al., 1993; Baukrowitz and Yellen, 1995; Ogielska and Aldrich, 1999); third, both are also slowed when the outer pore is occupied by tetraethylammonium (TEA) (Grissmer and Cahalan, 1989; Choi et al., 1991); fourth, mutation at a homologous position alters the function of both genes (Pardo et al., 1992; Lopez et al., 1993); fifth, a conserved negative charge before the P loop is key to both (Larsson and Elinder, 2000; Ortega-Saenz et al., 2000); and, sixth, cysteine substitutions known to mediate crosslinking in Shaker (418 and 452) (Larsson

[1] Correspondence: steve.goldstein@yale.edu

and Elinder, 2000) are similarly effective at homologous sites in KCNKØ (28 and 115). Finally, these conformational changes in KCNKØ are seen to be coupled to regulation from the cytoplasm.

The direct correspondence of KCNKØ activity and changes in the outer pore suggests the presence of a gate that reflects (and may mediate) opening and closing. A comparable mechanism may be operative across the 2-P-domain channel family as the yeast channel TOK1 and two mammalian variants, KCNK2 and KCNK3 (of the central nervous system and heart), show similar sensitivity to external permeant ions (Ketchum et al., 1995; Fink et al., 1996; Loukin et al., 1997; Vergani et al., 1998; Lopes et al., 2000, 2001; Bockenhauer et al., 2001). That the KCNKØ and VGK channel outer pores are functionally and structurally similar supports the idea that a gate that functions passively in VGK channels has been rendered dynamically responsive to cytoplasmic regulation in KCNKØ. The results indicate convergence of mechanism in divergent proteins and suggest that drugs or mutations that alter VGK channel C-type gating may offer a strategy to modify KCNK leak channel function in health and disease.

Results

External Zinc Blocks KCNKØ in an Activity-Dependent Manner

Zinc was identified as the most potent inhibitor of KCNKØ present in venom of the spider *Agelina labyranthica* (not shown). Applied from the bath, zinc reversibly inhibited KCNKØ channels expressed in *Xenopus laevis* oocytes and studied by two-electrode voltage clamp, showing half-block (IC_{50}) at 3.5 ± 1.5 μM with an apparent Hill coefficient ~1 (Figures 1A and 1B). Zinc inhibition was sensitive to channel activity level: the rate of block was ~9-fold slower when KCNKØ was pretreated with 50 nM PMA, a protein kinase C (PKC) activator that increased current density ~10-fold (Figure 1C). Supporting the idea that zinc does not block via a simple bimolecular interaction with an available site, the apparent on-rate (τ_{on}) was not linearly proportional to zinc concentration but increased only 2-fold with a 1000-fold elevation, from 1 to 1000 μM zinc (Figure 1D). A possible explanation for these findings was a rate-limiting change in channel conformation that exposed (or created) a zinc blocking site on the external face of the channel.

A Useful Deletion Mutant, ΔKCNKØ

We previously described a mutant (ΔKCNKØ) that lacks the regulatory carboxy-terminal residues 299–1001 of KCNKØ and is, therefore, unresponsive to kinase regulators but shows wild-type conductance and gating behavior; single ΔKCNKØ channels appear to visit the same states as full-length KCNKØ but with largely invariant frequency and duration (Zilberberg et al., 2000). Here, the stable attributes of ΔKCNKØ channels facilitated studies of zinc block at both the macroscopic and single channel levels. Thus, zinc block of KCNKØ varied with activity (Figure 1C) while ΔKCNKØ activity and zinc inhibition were stable over time and unaltered by PMA treatment (Zilberberg et al., 2000). Otherwise, zinc blocked ΔKCNKØ like the full-length channel, demonstrating an IC_{50} of 5.0 ± 1.0 μM and a Hill coefficient ~1 (mean ± SEM for 6 cells). Further, the rate and magnitude of inhibition of ΔKCNKØ by zinc were voltage independent from 0 to −100 mV (15 μM zinc, n = 6 cells) while increasing external potassium concentration from 0 to 100 mM (by isotonic replacement for sodium) decreased equilibrium inhibition by 15 μM zinc from 59 ± 3 to 29% ± 4% and slowed block kinetics from τ_{on} = 50 ± 7 to 85 ± 10 s (mean ± SEM for 6 cells, approximated by a single exponential, Figure 1E).

Zinc Block Reports a State Change

Single KCNKØ channels move in a regulated fashion between a long-lived open burst configuration (containing one open and three closed times) and a long-lasting closed state, C_{long} (Zilberberg et al., 2000). Application of PMA leads KCNKØ channels to spend more time in the open burst state due to a decrease in the frequency and duration of visits to C_{long}. That zinc block of full-length channels was infrequent after PMA treatment (Figure 1C) suggested block did not occur until channels had left the open state.

To assess further, single ΔKCNKØ channels were studied in on-cell mode, to eliminate the confounding effects of both regulation and "run-down" (Zilberberg et al., 2000; Ilan and Goldstein, 2001), with various levels of zinc in the pipette. Representative traces show that zinc reduced single channel open probability (Po) from 0.66 ± 0.05 (control) to 0.07 ± 0.02 (100 μM zinc) without an effect on unitary current, which was 3.2 ± 0.1 pA at all zinc concentrations (Figure 2A and Table 1). Quantification of dwell times suggested that zinc did not alter channel behavior during open bursts as no difference was detected in mean intraburst open time (O_{time}) or dwell time for any of the short closed states (C_{short1}, C_{short2}, C_{short3}; Table 1). Conversely, zinc decreased the frequency of the long-closed state C_{long} (mean duration ~6 s) from 18% ± 2% to 7% ± 1% of closures (filtered at 50 Hz) and led to emergence of a new nonconducting state lasting ~50 s, C_{Zn} (Figure 2D, arrow, Table 1).

As PMA treatment of full-length channels both slowed zinc block kinetics and increased occupancy of O_{burst}, we sought to further evidence for this relationship. Indeed, rates of zinc inhibition correlated inversely with time spent in the open burst state: longer openings resulted in less efficient blockade (Figure 2E). Channels displaying five different mean open burst times were studied: KCNKØ, ΔKCNKØ, another deletion variant with residues 619–1001 removed (ΔΔKCNKØ), a ΔKCNKØ point mutant (S112Y), and KCNKØ activated with PMA. A strict relationship was observed between single channel O_{burst} duration and the apparent macroscopic forward rate constants for zinc blockade, τ_{on} (Figure 2E, Pearson product-moment correlation coefficient 0.99 significant at the 0.01 level by 2-tailed analysis). Conversely, τ_{on} showed no correlation with the duration of C_{long} (Figure 2F). These findings supported the conclusion that zinc blocked after the channel exited the open burst state.

Histidine 29 Is Required for Zinc Block

KCNKØ residues required for zinc blockade were sought as follows. Involvement of a histidine was implicated because inhibition was almost eliminated by lowering

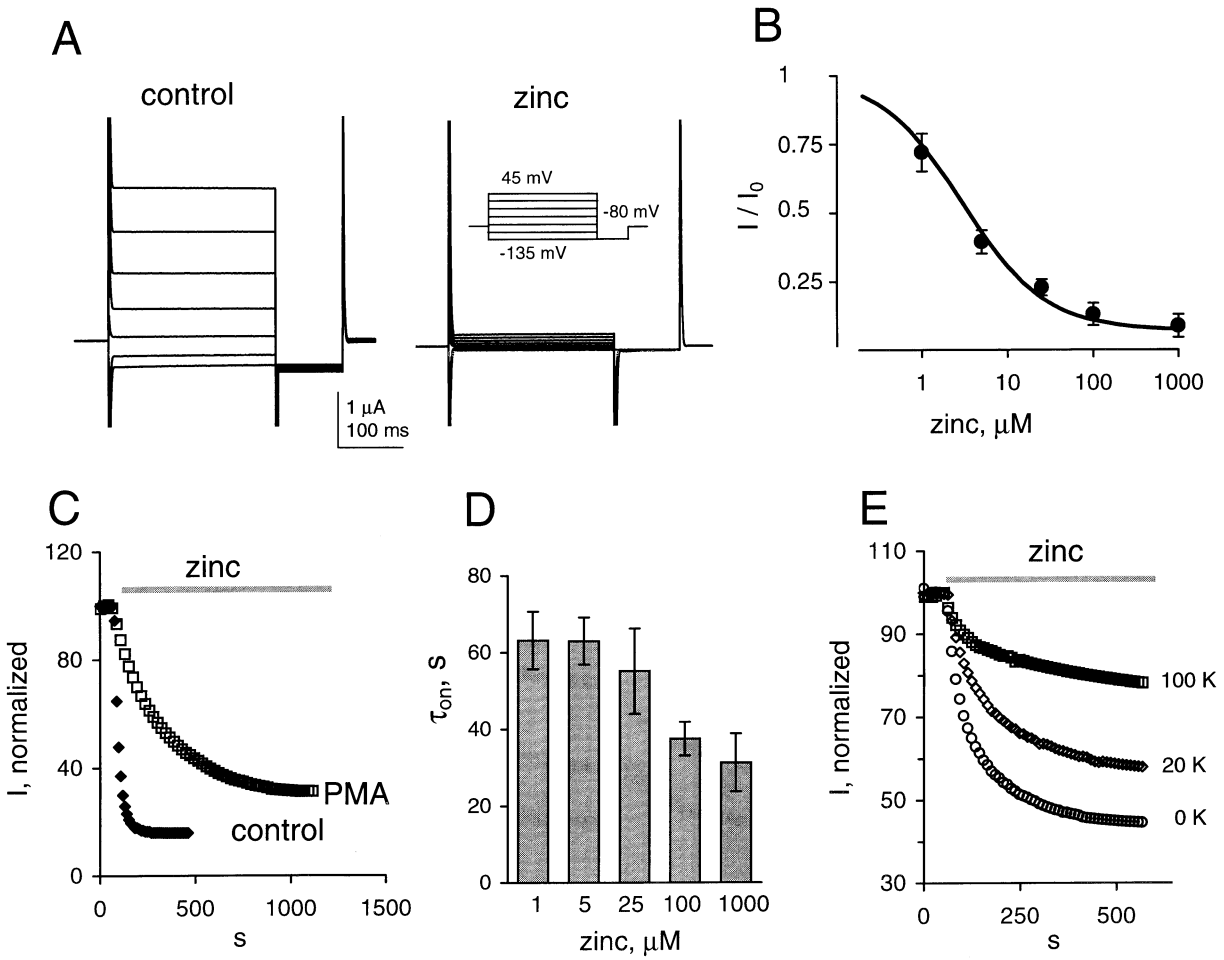

Figure 1. KCNKØ Channels Are Inhibited by Externally Applied Zinc

Macroscopic currents measured by two-electrode voltage clamp.

(A) Raw current traces for a representative oocyte expressing KCNKØ channels and bathed in 5 mM potassium solution without (control) or with 100 μM zinc (zinc). The cell was held at −80 mV, pulsed for 250 ms from −135 to 45 mV in 30 mV steps and then for 75 ms at −135 mV; 2 s interpulse interval.

(B) Dose-response for zinc inhibition of KCNKØ channels in 5 mM potassium solution at 30 mV by the protocol in panel (A). Data points are mean ± SEM for five cells. The solid line is a fit of the data to the equation: $I = 1 / (1 + ([Zn^{2+}]/K_{1/2})^h)$ where I is the measured current, $K_{1/2}$ is the concentration of Zn^{2+} required to achieve 50% inhibition, and h is the Hill coefficient. $K_{1/2}$ was 3.5 ± 1.5 μM zinc and h was 0.95 ± 0.07.

(C) Representative KCNKØ current magnitude during application of 100 μM zinc under control conditions and after 15 min treatment with 50 nM PMA, as indicated. There was a 9 ± 2-fold increase in the time constant for inhibition with PMA compared to control conditions (from 30.8 ± 7.0 to 271 ± 72 s, mean ± SEM, n = 10 cells). Equilibrium inhibition was reduced by PMA from 85% ± 5% to 65% ± 26% (mean ± SEM, n = 10 cells).

(D) Rate of inhibition of KCNKØ channels (τ_{on} in s) at different zinc concentrations using 5 mM potassium solution, a holding voltage of −80 mV, and 200 ms pulses to 25 mV (mean ± SEM, n = 5 cells). Time constants were calculated by fitting the data to the equation $I = I_0 + A^*e^{-T/\tau}$ where I is the measured current, I_0 is the blocked current at equilibrium, T is the elapsed time after zinc application, τ_{on} is the apparent forward time constant in seconds, and A is a constant (Experimental Procedures). Unblock τ_{off} was 32 ± 4 s, 45 ± 6 s, 58 ± 6 s, to 85 ± 9 s with zinc at 1, 5, 25, and 100 μM, n = 6–8 cells. Solution exchange required 4 ± 0.2 s as assessed by the change in current on exchange of 5 for 100 mM potassium solution (n = 4 cells).

(E) External potassium alters zinc inhibition. Representative ΔKCNKØ currents from a cell exposed to 15 μM zinc at the indicated potassium concentration. Oocytes were held at −80 mV and stepped to 25 mV for 200 ms with a 10 s interpulse interval. Plotted as fraction of unblocked current for each potassium concentration.

external pH to 5.5 or when cells were pretreated with diethyl pyrocarbonate (0.1% DEPC), a reagent that covalently modifies the imidazole ring of histidine (not shown). Thereafter, individual point mutation of H26, H94, H165 (and C73 and C103) was found to have no effect on inhibition whereas altering H29 to asparagine (H29N) or serine (H29S) produced channels markedly insensitive to zinc (Figures 3A and 3B). This site is predicted to lie on the external face of the channel in the first extracellular loop (Figure 3A).

These attributes of KCNKØ inhibition by zinc were reminiscent of findings with the VGK channel Shaker (after mutation to yield cysteine in the outer pore) that supported a model for C-type inactivation involving rearrangement of residues in the external pore mouth based on consideration of state-dependent cadmium

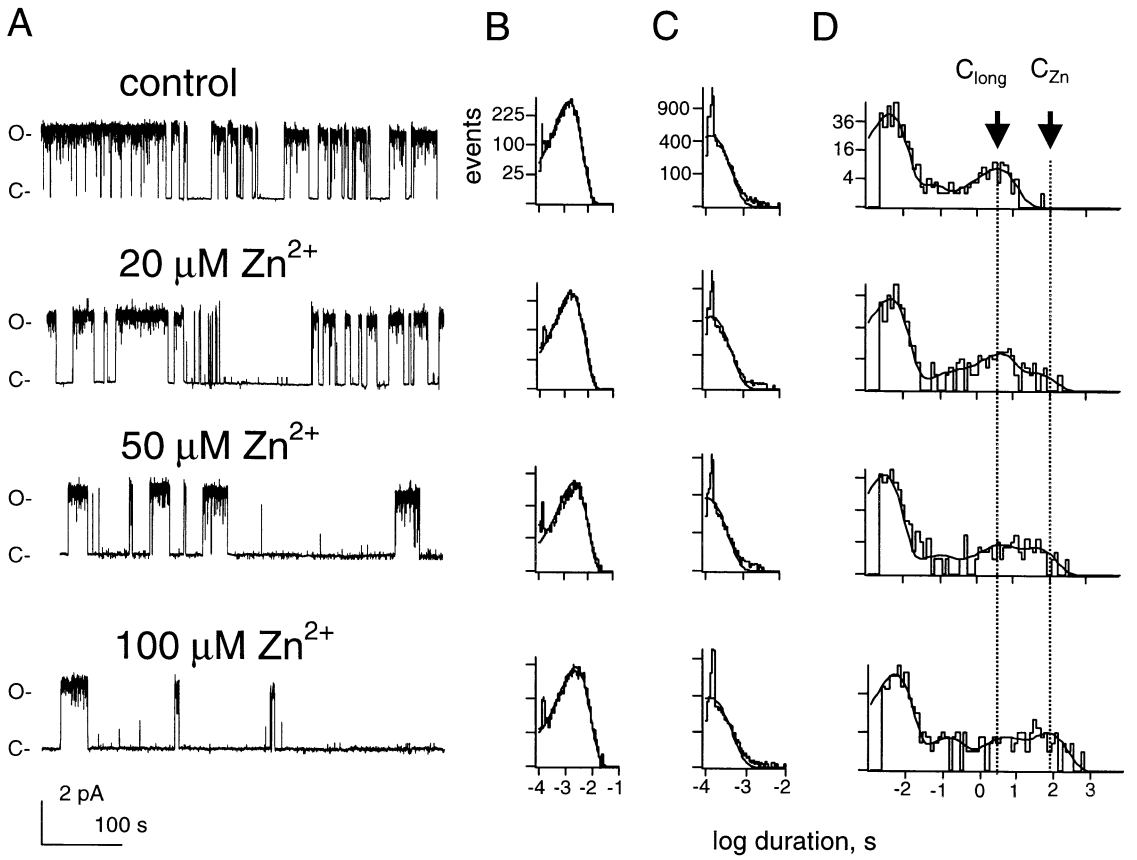

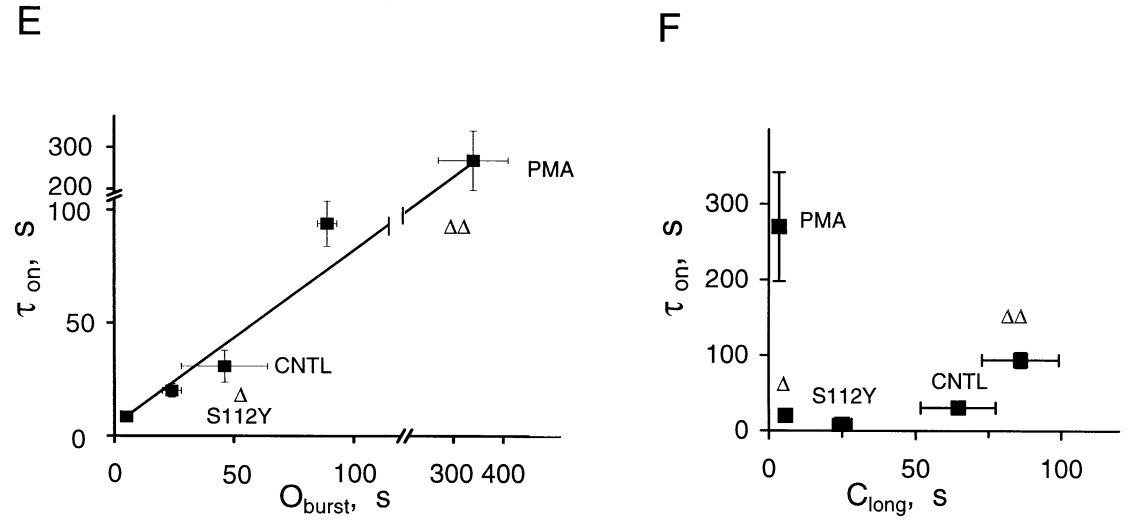

Figure 2. Zinc Does Not Block during O_{burst}

Single ΔKCNKØ channels were studied in on-cell patches at 60 mV with 140 mM potassium solution in the pipette (control) or with increasing zinc, as indicated. Values are reported in Table 1.

(A) Representative single channel traces, sampled at 940 Hz, filtered at 20 Hz. Open (O) and closed (C) state levels are indicated.

(B) Open time histograms from ~20 s (3–5 records). Sampled at 20 kHz, filtered at 3 kHz.

(C) Closed time histograms from ~20 s of data as in panel (B).

(D) Closed time histograms of 23–61 min of single channel data sampled at 940 Hz and filtered at 50 Hz (n = 3–5 channels). Arrow indicates closure associated with zinc, C_{Zn}.

(E) Macroscopic time constant for zinc inhibition (τ_{on}) versus single channel O_{burst} duration. Whole-cell measurements in 20 mM potassium solution with 100 μM zinc using a holding voltage of −40 mV and 200 ms pulses to 25 mV; τ_{on} was determined as in Figure 1D (mean ± SEM, n = 6–8 cells). Single channels were studied on-cell at 60 mV with 140 mM potassium solution in the bath and pipette, sampled at 940 Hz,

Table 1. Gating Parameters for Single ΔKCNKØ Channels with and without Zinc

	Time (min)	Po	O_{burst} (s)	C_{long} (s)	C_{Zn} (s)	O_{time} (ms)	C_{short1} (ms)	C_{short2} (ms)	C_{short3} (ms)
Control	23	0.66 ± 0.05	15 ± 2	3.85 ± 0.35	—	1.9 ± 0.2	58 ± 20	5.5 ± 0.6	0.15 ± 0.02
20 μM zinc	23	0.38 ± 0.04	9 ± 1	3.95 ± 0.27	38.0 ± 4.2	1.7 ± 0.4	150 ± 43	5.2 ± 0.3	0.13 ± 0.03
50 μM zinc	37	0.24 ± 0.03	11 ± 2	4.11 ± 0.31	42.8 ± 3.3	1.6 ± 0.2	87 ± 25	4.6 ± 0.5	0.17 ± 0.03
100 μM zinc	61	0.07 ± 0.02	6 ± 2	3.01 ± 0.36	66.3 ± 4.5	2.0 ± 0.3	129 ± 39	6 ± 0.5	0.15 ± 0.01

Parameters obtained by fitting dwell times distributions for three patches with a single KCNKØ channel by a half-amplitude criterion and a binned maximum likelihood method (Experimental Procedures). P_o, O_{burst}, C_{long}, C_{short1}, C_{short2}, and C_{Zn} obtained with long records filtered at 50 Hz, sampled at 940 Hz. O_{time} and C_{short3} determined by analysis of 20 s portions of intraburst recordings sampled at 20 kHz filtered at 3 kHz. O_{burst} determined from open bursts flanked by closures lasting over 1 s. P_o calculated from the burst probability and the intraburst P_o (0.92 ± 0.01 for all zinc concentrations, filtered at 3 kHz). The data support the conclusion that zinc blocks after channels exit O_{burst}. Reduction in O_{burst} duration is attributed to block of C_{long} events shorter than the defined cutoff (1 s).

block (Yellen et al., 1994) and chemical modification (Liu et al., 1996). Furthermore, interaction of zinc with KCNKØ via H29 appears to depend on a change in the outer pore and the homologous residue in Shaker (A419) alters its local environment during C-type gating (Loots and Isacoff, 2000). A direct comparison of previously reported attributes of Shaker C-type inactivation and KCNKØ gating was thus undertaken and marked similarities were revealed.

The O_{burst} to C_{long} Transition in KCNKØ Is Similar to VGK C-Type Gating

I. External Potassium

The effects of bath potassium were studied because external permeant ion slows VGK channel C-type inactivation (Lopez et al., 1993; Baukrowitz and Yellen, 1995, 1996; Ogielska and Aldrich, 1999). Single ΔKCNKØ channels in on-cell patches with 140 mM potassium in the pipette demonstrated a probability of being in the open burst state (P_{burst}) of 0.73 ± 0.07 (Figure 4, Table 2). When the pipette contained 140 mM sodium or NMDG solution, P_{burst} was reduced to 0.32 ± 0.05 and 0.24 ± 0.04, respectively; this was due to decreased open burst time (O_{burst}) and increased C_{long} duration (Figure 4, Table 2). Conversely, channel behavior within open bursts was similar with potassium or sodium in the pipette: no difference was detected in mean open time or dwell times for any of the three intraburst closed states (Table 2). With NMDG in the pipette, a small increase in frequency of the shortest intraburst closure (C_{short3}) yielded an ~23% decrease in mean open time (Table 2). Thus, the effects of external permeant ion on C_{long} and C-type gating were similar.

II. External TEA

As VGK channel C-type inactivation is slowed when the pore is blocked by tetraethylammonium (TEA) (Grissmer and Cahalan, 1989; Choi et al., 1991), this agent was next employed and found to have similar effects on C_{long}. KCNKØ channels were inhibited by external TEA with low affinity: 95 mM TEA blocked 45% ± 5% of whole-cell outward current at 60 mV (n = 10 cells, not shown). Single ΔKCNKØ channels were assessed in on-cell mode with 60 mM potassium and either 80 mM sodium or 80 mM TEA in the pipette. Compared to sodium, TEA had two marked effects: it reduced apparent single channel conductance and increased open burst probability (Figure 5A and Table 2). Single channel conductance at 60 mV was decreased by TEA from 3.5 ± 0.2 to 2.8 ± 0.2 pA (mean ± SEM, n = 5, filter frequency 3 kHz, sample rate 20 kHz), consistent with a failure to resolve fast blocking events. In addition, TEA increased the frequency of a nonconducting state with a mean dwell time of 4.5 ± 0.7 ms leading to an ~2-fold decrease in mean open time (Figures 5B–5D and Table 2).

Perhaps, the most dramatic effect of TEA was on KCNKØ channel gating: the blocker suppressed visits to C_{long} (Figures 5A and 5D) to produce an ~4-fold increase in O_{burst} and an increase in P_{burst} from 0.74 ± 0.06 to 0.85 ± 0.05 (Table 2). Consistent with the conclusion that zinc blocks after channels exit the O_{burst} state, TEA slowed the macroscopic inhibition rate constant for zinc inhibition from 19.5 ± 1.2 s to 50.0 ± 9.1 s (95 mM TEA in 5 mM potassium solution, mean ± SEM, n = 6).

III. A Homologous Site

In Shaker, mutation of an external threonine (T449) just following the P loop in the primary sequence alters C-type gating kinetics (Lopez et al., 1993); this is also observed at an analogous position with Kv1.4 (Pardo et al., 1992) and may result from changes in potassium occupancy of the outer pore vestibule. We therefore mutated the homologous site after the first P loop in ΔKCNKØ from serine to tyrosine (S112Y) and results were as expected. The mutant channel showed no change in either its selectivity for potassium over sodium (as assessed by whole-cell reversal potentials at varying external potassium concentrations) or instantaneous current development with voltage steps (not shown). In contrast, single S112Y channels showed an ~4.5-fold increase in C_{long} (with an ~5-fold decrease in O_{burst}) while intraburst open and closed state dwell times were unaffected (Figures 5B–5D, Table 2). Moreover, as expected,

filtered at 50 Hz (mean ± SEM, n = 3–5 channels). O_{burst} was determined as described in Table 1. Channels and conditions: KCNKØ under control conditions (CNTL); KCNKØ treated with 50 nM PMA (PMA); ΔKCNKØ channels (Δ); ΔKCNKØS112Y (S112Y); a deletion mutant lacking residues 619–1001 ΔΔKCNKØ (ΔΔ). The linear regression is described (Results).
(F) Macroscopic time constant for zinc inhibition (τ_{on}) does not correlate with C_{long} duration, studied as in panel (A).

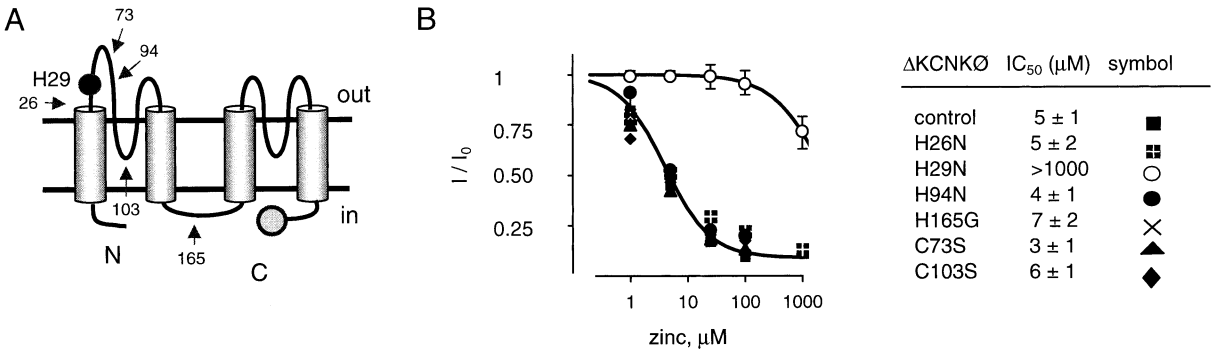

Figure 3. Histidine 29 Is Required for Zinc Blockade

(A) Predicted membrane topology of a KCNKØ subunit indicating the two P domains and four transmembrane segments; black circles indicate histidine 29 (H29) while arrows note other histidine residues (positions 26, 94, 165) and two cysteines (positions 73, 103). The carboxyl terminus (700 amino acids, gray circle) is lacking in ΔKCNKØ channels.

(B) Dose-response relationships for zinc inhibition of ΔKCNKØ (control) and six ΔKCNKØ variants carrying point mutations at single histidine or cysteine residues. Channels were studied and data analyzed as in Figure 1B. Data points represent the mean of 5–7 cells. For clarity, error bars (±SEM) are indicated only for control and H29N channels. Hill coefficient for the control channel was 1.05 ± 0.06. IC_{50} values for zinc inhibition of the control and mutant channels are indicated (mean ± SEM).

the rate of inhibition (100 μM zinc, 20 mM potassium solution) was faster with the mutant (S112Y, τ_{on} = 8.8 ± 1.1 s, n = 6 cells) than in S112 channels (τ_{on} = 25.1 ± 2.0 s, n = 5 cells).

IV. A Conserved Charge

An extracellular glutamate found in most VGK and KCNK subunits before each P loop was found to be key to C-type gating in Shaker channels when its mutation to glutamine (E418Q) (Ortega-Saenz et al., 2000) or cysteine (E418C) (Larsson and Elinder, 2000) yielded significant acceleration of C-type inactivation; the negative charge on Shaker E418 appeared to interfere with entry into the C-type state. Similar observations were made when the homologous residue in KCNKØ (E28) was altered. Thus, ΔKCNKØ E28C (Figure 6A) showed an ~5-fold decrease in macroscopic current magnitude compared to E28 channels that was revealed by single channel studies to be due to a 7-fold decrease in unitary P_o (secondary to a shortened open burst duration, Figure 6C and Table 2) offset by an increase in unitary current size (from 3.2 ± 0.1 to 3.8 ± 0.2 pA at 60 mV, mean ± SEM, n = 7).

As with Shaker channels, the effects of the E28C mutation were reversed by covalent modification to restore a negative charge at the site. Reaction of ΔKCNKØ E28C with the thiol-specific reagent methanethiosulfonate ethylsulfonate (MTSES) increased macroscopic current 4.4 ± 0.4-fold (mean ± SEM, n = 8; Figure 6B) while having no effect on E28 channels (Figure 6B, right). At the single channel level, the current increase was seen to result from an increase in P_o due to increased open burst duration and decreased C_{long} dwell time (Figure 6D and Table 2). These effects of MTSES were also observed with full-length KCNKØ E28C channels which showed a 3.0 ± 0.3-fold increase in macroscopic current (mean ± SEM, n = 8 cells) whereas E28 channels were unchanged by treatment with the reagent.

As expected, the E28C mutation which decreased O_{burst} and increased C_{long} also speeded the time course for zinc inhibition compared to E28 channels (τ_{on} = 3.5 ± 0.3 s versus 20 ± 0.2 s, respectively, in 5 mM potassium solution) while MTSES application almost restored wild-type block kinetics (τ_{on} = 16.6 ± 2.4 s, Figure 6E). Studies of the homologous position preceding the second P domain in KCNKØ were not possible as E200C channels passed no current.

V. Sites that Interact in Shaker during C-Type Gating Predict Positions that Can Crosslink in KCNKØ

As the effects of potassium, TEA, mutation, and modification supported similarity of KCNKØ C_{long} and the Shaker C-type inactivated state, evidence for structural homology in the outer pore regions of the two channels was sought. Shaker E418 is in the fifth transmembrane segment (S5) and has been argued to interact within the same subunit near G452 and V451 in S6 to stabilize the C-type inactivation gate in the open conformation; this was reasoned because disulfide bonds could form between cysteine residues substituted at positions 418 and 452 or 418 and 451 to hold the gate static (Larsson and Elinder, 2000). Proximity of these sites in Shaker was suggested by interaction of analogous sites in the crystal structure of the bacterial KcsA channel where E51 is predicted to form hydrogen bonds with the backbone amides of T85 and V84 and the side chain hydroxyl of T85 (Figure 7A, dashed lines) (Doyle et al., 1998). Supporting strong relatedness with the Shaker pore, cysteine substitution at two homologous sites in KCNKØ specifically yielded a channel closed by disulfide bond formation and opened by reductive lysis of the bond.

Initially, currents carried by the double mutant ΔKCNKØ E28C, T115C (Figure 7B), analogous to Shaker E418C, G452C, were quite small. Upon bath application of the reducing agent dithiothreitol (DTT, 5 mM), current magnitude increased 4.0 ± 0.4-fold (Figure 7B, period 1) even after the agent was washed away (mean ± SEM, n = 7; Figure 7B, period 2). Subsequent application of the oxidizing agent 5,5-dithio-bis(2-nitrobenzoic acid) (DTNB, 0.5 mM) decreased current to its initial level (Figure 7B, period 3) and this change was also resistant

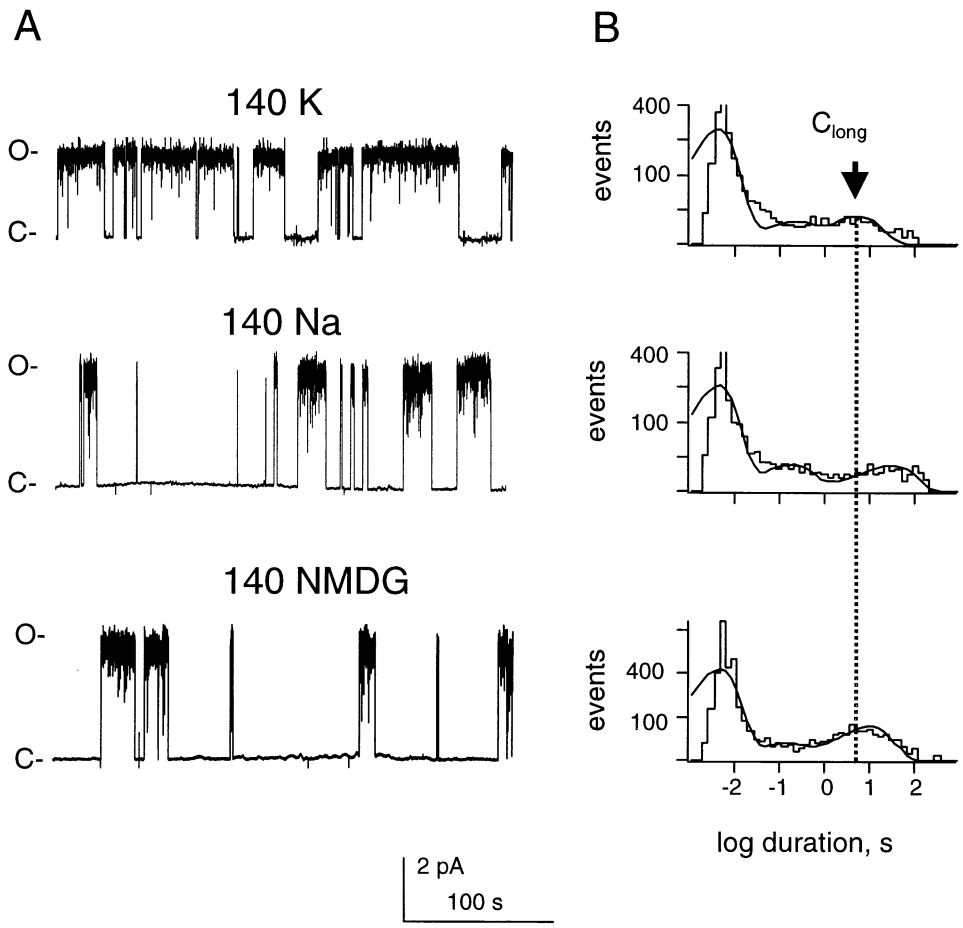

Figure 4. External Potassium Inhibits Long Closures

Single ΔKCNKØ channels in on-cell patches at 60 mV with 140 mM potassium in the bath and 140 mM potassium, sodium, or NMDG solution in the pipette. Values in Table 2.

(A) Representative single channel traces sampled at 500 Hz, filtered at 20 Hz. Open (O) and closed states (C) levels are indicated.

(B) Closed time histograms for single channels with different external solutions sampled at 500 Hz, filtered at 50 Hz. Data from 59–117 min (n = 4–6 channels).

to reagent wash out (Figure 7B, period 4). Oxidation-induced current suppression could then be reversed by reapplication of DTT (Figure 7B, period 5). The oxidizing mixture copper/phenanthroline (4/200 μM) had similar effects as DTNB (not shown). These findings suggested that E28C and T115C could form a disulfide bond spontaneously, that the bond was broken by chemical reduction, and then reformed by oxidation. In support for

Table 2. Single Channel Gating Parameters

Channel Condition	Time (min)	Po	O_{burst} (s)	C_{long} (s)	P_{burst}	O_{time} (ms)	C_{short1} (ms)	C_{short2} (ms)	C_{short3} (ms)
ΔKCNKØ									
140K	63	0.67 ± 0.06	25 ± 4	5.6 ± 0.4	0.74 ± 0.07	2.2 ± 0.4	140 ± 25	5.3 ± 0.6	0.17 ± 0.02
140 Na	59	0.29 ± 0.04	14 ± 2	31 ± 3.0	0.32 ± 0.05	2.1 ± 0.3	133 ± 39	5.5 ± 0.5	0.16 ± 0.03
140 NMDG	117	0.21 ± 0.03	5.1 ± 0.7	8.5 ± 1.5	0.24 ± 0.04	1.7 ± 0.5	121 ± 39	5.6 ± 0.5	0.17 ± 0.01
60 K/80 Na	62	0.67 ± 0.06	24 ± 5	5.5 ± 0.4	0.73 ± 0.07	2.1 ± 0.3	152 ± 43	4.5 ± 0.3	0.17 ± 0.03
60 K/80 TEA	95	0.64 ± 0.05	90 ± 6	7.0 ± 2.1	0.85 ± 0.05	1.0 ± 0.2	98 ± 21	4.5 ± 0.7[a]	0.24 ± 0.04[a]
ΔKCNKØ S112Y									
140 K	101	0.25 ± 0.02	5.0 ± 0.7	25 ± 3.2	0.27 ± 0.03	1.9 ± 0.4	96 ± 21	4.2 ± 0.4	0.15 ± 0.01
ΔKCNKØ E28C									
140 K	64	0.09 ± 0.02	1.2 ± 0.4	8.8 ± 2.1	0.10 ± 0.02	2.6 ± 0.4	95 ± 20	6.0 ± 0.5	0.16 ± 0.03
140 K/MTSES	113	0.52 ± 0.09	6.2 ± 0.5	1.5 ± 2.1	0.61 ± 0.11	2.5 ± 0.4	89 ± 31	6.9 ± 0.8	0.15 ± 0.03

Kinetics parameters were determined as in Table 1. Four to six single channels were used for the long closure analyses. P_{burst}, probability the channel is in the burst mode. Condition indicates solution in the pipette.

[a] n.b., in the presence of TEA, C_{short1} and C_{short2} dwell times are contaminated by TEA blocking events of similar duration.

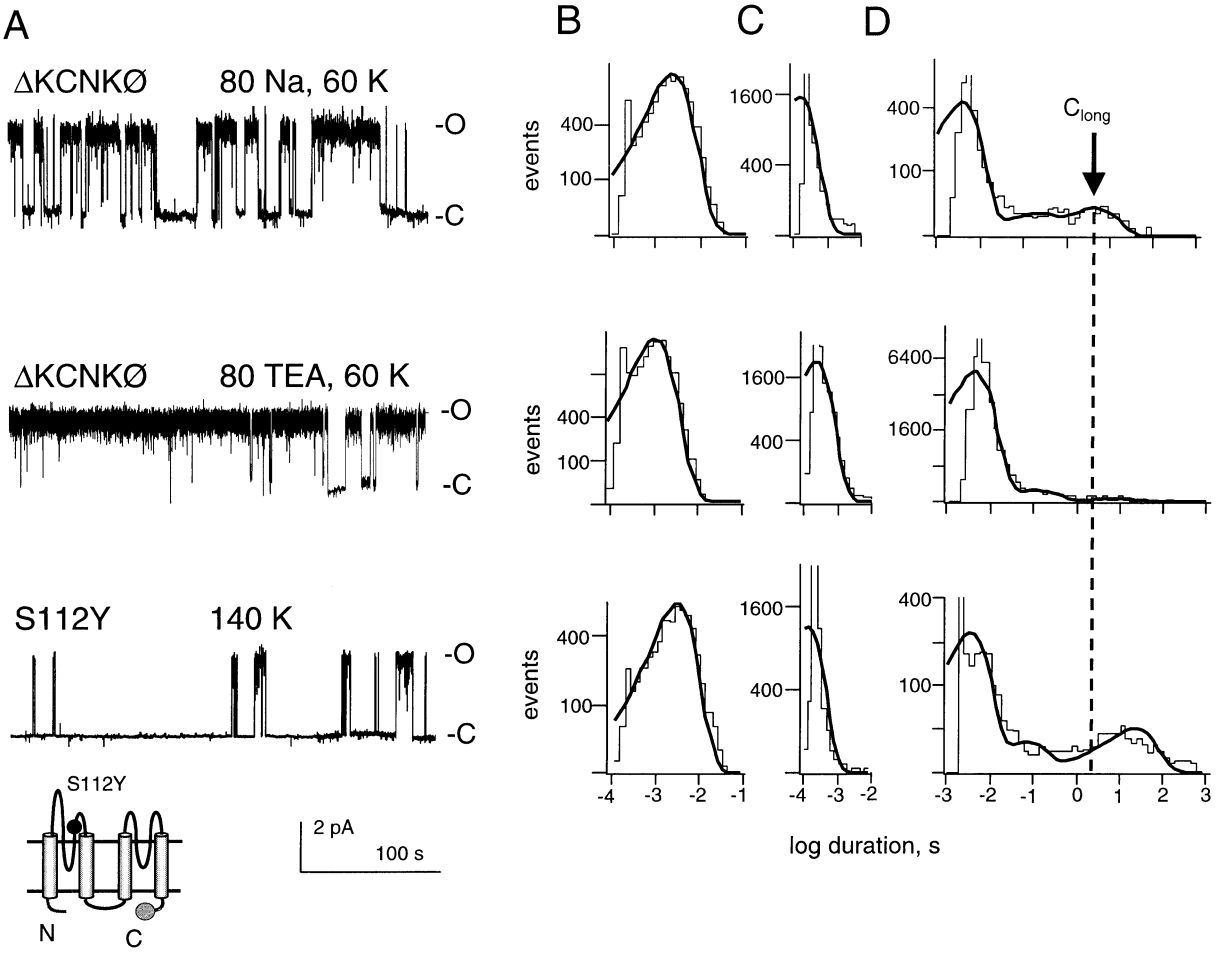

Figure 5. External TEA Inhibits Long Closures (while a Pore Mutation Favors the State)

Single ΔKCNKØ and ΔKCNKØ S112Y channels were studied in on-cell patches at 60 mV with 140 mM potassium solution in the bath. Values in Table 2.

(A) Representative single channel traces sampled at 500 Hz and filtered at 20 Hz of ΔKCNKØ channels with 80 mM NaCl and 60 mM KCl in the pipette; ΔKCNKØ channels with 80 mM TEA and 60 mM KCl in the pipette; ΔKCNKØ S112Y channels with 140 mM KCl in the pipette. Open (O) and closed states (C) levels are indicated.

(B) Open time histograms from ~20 s (4 records). Data sampled at 20 kHz, filtered at 3 kHz.

(C) Closed time histograms from ~20 s of data, as in panel (B).

(D) Closed time histograms of 62–101 min of single channel recordings sampled at 500 Hz, filtered at 50 Hz (n = 4–5 channels); arrow indicates C_{long}.

this idea, small initial currents passed by KCNKØ E28C, T115C channels were little affected by application of the oxidizing agent DTNB (Figure 7C, period 2), but after DTT augmentation (Figure 7C, period 3), DTNB could suppress the current (Figure 7C, period 4).

These effects of DTT and DTNB were specific for KCNKØ channels bearing both E28C and T115C mutations; thus, no effect of either agent was observed with wild-type KCNKØ channels (Figure 7D, inset), nor channels with only the E28C or the T115C mutation (Figure 7D). Moreover, coexpression of E28C subunits and T115C subunits also yielded currents that were insensitive to DTT and DTNB, indicating that both cysteines had to flank the same P loop to crosslink (Figure 7D). Finally, T115C was unique in its collaboration with E28C as A112C, P113C, T114C, and F116C did not mimic these effects (Figure 7D). These results support the conclusion that, as with Shaker E418 and G452, and KcsA E51 and T85, KCNKØ E28 and T115 are in close proximity (Figure 7A).

Relationship to Regulated Activity

KCNKØ activity is regulated by phosphorylation of the intracellular carboxyl terminus to alter the frequency and duration of C_{long}; thus, the nonselective, kinase inhibitor staurosporine drives single KCNKØ channels into C_{long} (Zilberberg et al., 2000). As block of KCNKØ by TEA (Figure 5) and MTSES modification of KCNKØ E28C (Figure 6) could change the attributes of C_{long} from the external face of the channel, we sought to determine if internal and external modifiers of channel function were independent or related. Just as external TEA suppressed natural excursions into C_{long} (Figures 5A and 5D, Table 2), so it antagonized staurosporine-induced entry into

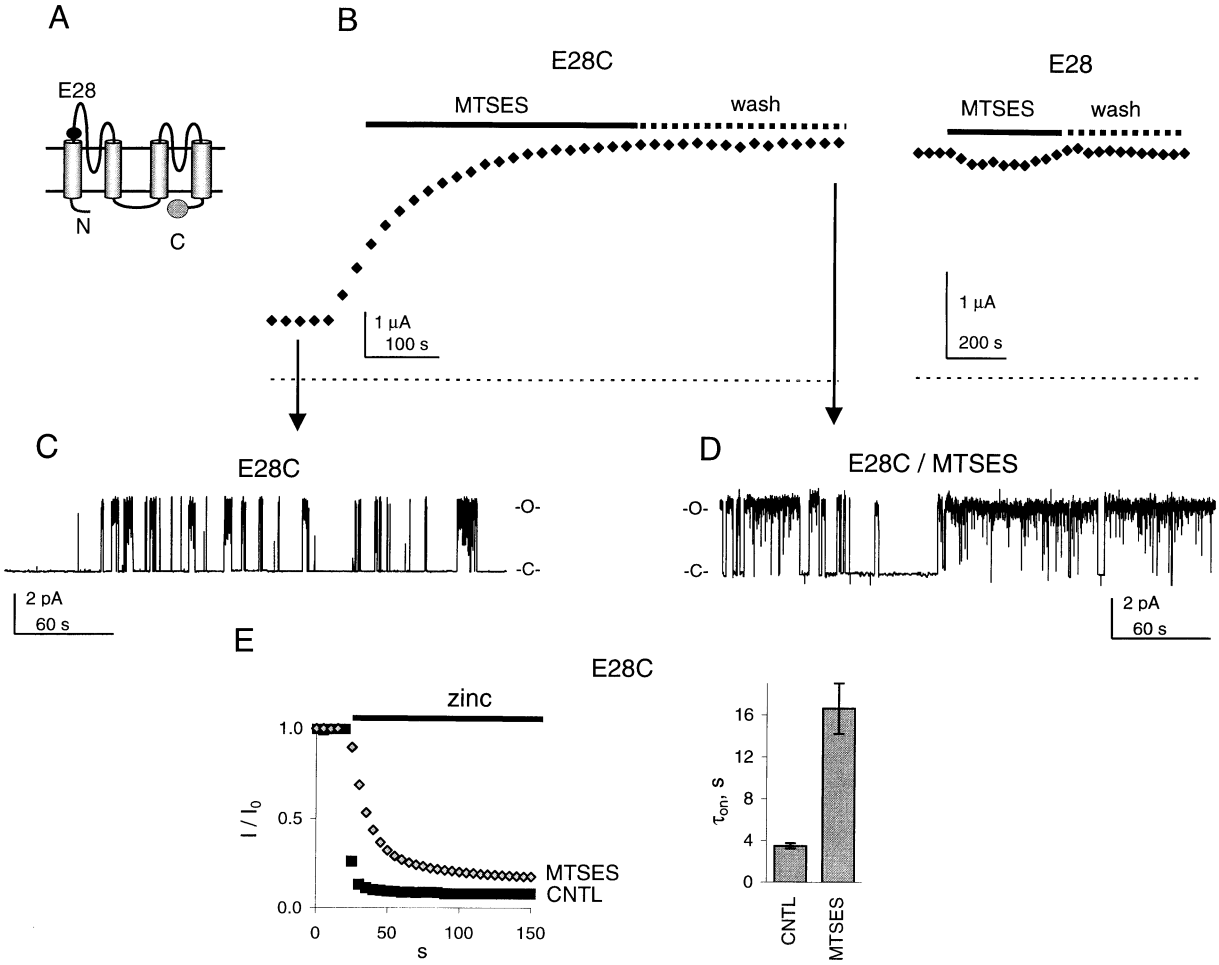

Figure 6. A Negative Charge at Position 28 Is Required to Maintain the Open State

(A) Predicted topology of ΔKCNKØ; black circle indicates the glutamate at position 28 (E28).

(B) Macroscopic current passed by a cell expressing ΔKCNKØ E28C channels (left) or wild-type ΔKCNKØ (E28) channels (right); measured by two-electrode voltage clamp, before and during application of 5 mM MTSES (solid bar) in 5 mM potassium solution and a subsequent wash with 5 mM potassium solution (dashed bar). Cells were held at −80 mV and stepped to 25 mV for 200 ms with a 10 s interpulse interval, every second point is plotted. Thin dashed line indicates zero current level.

(C) A single ΔKCNKØ E28C channel trace studied in an on-cell patch at 60 mV with 140 mM potassium solution in the pipette; sampled at 500 Hz and filtered at 20 Hz. Open (O) and closed (C) state levels are indicated. Kinetics values reported in Table 2.

(D) A single ΔKCNKØ E28C channel trace after 10 min exposure to 5 mM MTSES and 2 min in control solution, as in (B) (left). Open (O) and closed (C) state levels are indicated. Kinetic values reported in Table 2.

(E) Zinc inhibition of ΔKCNKØ E28C currents is slower after MTSES application. Left: current passed by a cell expressing ΔKCNKØ E28C channels during application of 100 μM zinc in 5 mM potassium solution before (CNTL) and after 5 min incubation with 5 mM MTSES. Cells were held at −80 mV and stepped to 25 mV for 200 ms with a 5 s interpulse interval. Right: inhibition by 100 μM zinc for six cells expressing ΔKCNKØ E28C channels (τ_{on} in s, values in Results) before (CNTL) and after MTSES as in left panel, fit as in Figure 1D (mean ± SEM).

the state (Figure 8A). Oocytes expressing wild-type KCNKØ were first partially deactivated by exposure to staurosporine (2 μM) for 3 min; then, in the continued presence of staurosporine, the channels were blocked by 95 mM external TEA for 100 s; only after TEA was washed away did staurosporine-mediated current deactivation continue. By this protocol, KCNKØ current after exposure to TEA for 100 s was 94% ± 5% of pretreatment levels (mean ± SEM, n = 7) while it was 55% ± 6% after a 100 s wash in the absence of the blocker (mean ± SEM, n = 10). Similarly, activation of full-length KCNKØ E28C channels by PMA (Table 2) limited the enhancing effects of external MTSES as if the active conformation had already been achieved (Figure 8B). Thus, suppression of C_{long} by the external blocker interfered with intracellular downregulation while intracellular activation preempted upregulation by the external modifying agent. These observations supported the idea that conformational changes in the external pore resulted from cytoplasmic regulatory events.

Discussion

This work supports the conclusion that KCNKØ moves between open and closed states in direct correspondence to conformational changes in the external pore.

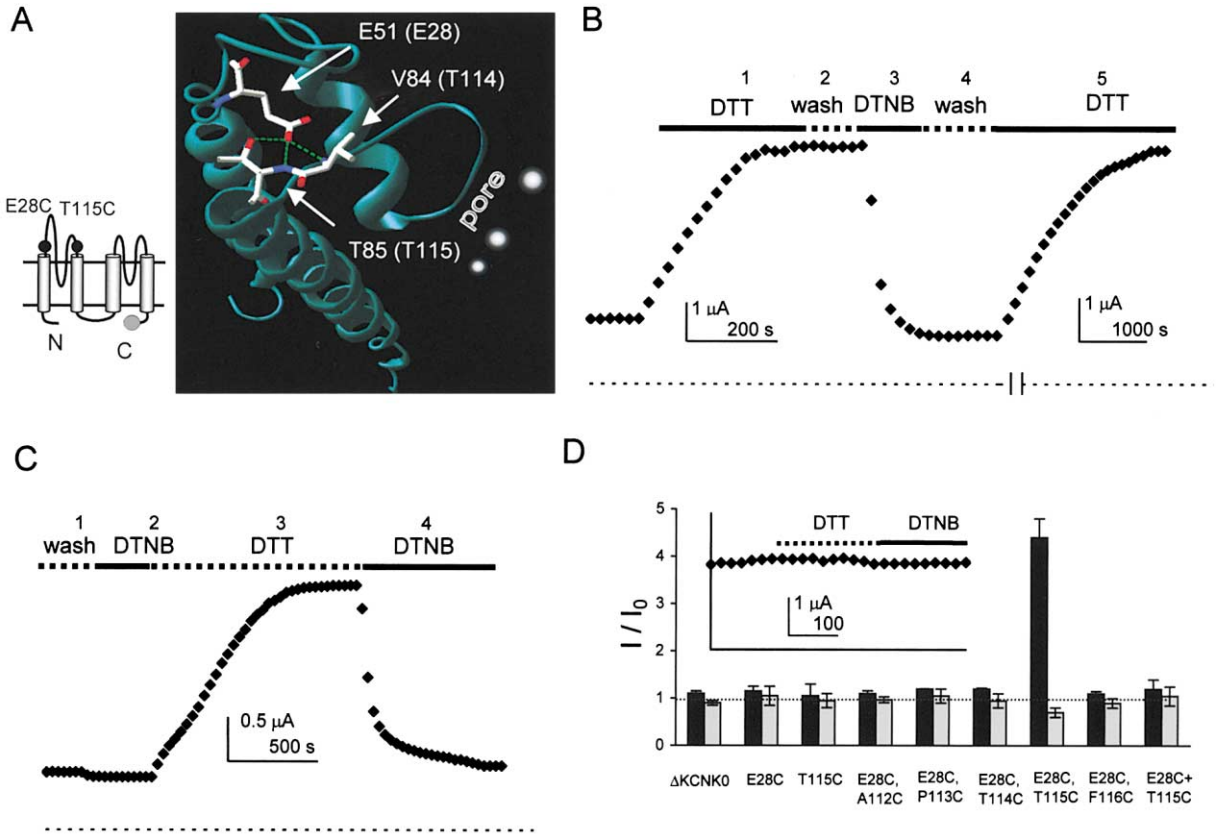

Figure 7. E28C Can Be Paired with T115C to Create a Disulfide Bond

(A) Left: predicted topology of ΔKCNKØ; black circles indicate the native glutamate and threonine at positions 28 (E28) and 115 (T115). Right: interactions predicted at homologous sites in KcsA are indicated in a view of the reported structure (Doyle et al., 1998); KcsA residues E28, V84, and T85 (arrows) align in the primary sequence with ΔKCNKØ residues E28, T114, and T115. The side chain of KcsA E51 is predicted to form hydrogen bonds (dashed lines) to the backbone amides of V84 and T85 and the side chain hydroxyl of T85. The structure was displayed using Swiss PdbViewer software (http://www.expasy.ch/spdbv/).

(B) Representative current passed by a cell expressing ΔKCNKØ E28C, T115C channels, studied by two-electrode voltage clamp with 5 mM potassium solution (control solution). The cells were perfused with the following solutions for the indicated time periods: 5 mM DTT for 420 s (solid bar), control solution for 140 s (wash), 0.5 mM DTNB (solid bar) for 160 s, control solution for 140 s (wash), and 5 mM DTT for 2200 s (solid bar). The oocyte was held at −80 mV and stepped to 25 mV for 200 ms with a 10 s interpulse interval. For the first 920 s, every second point is plotted; for the second DTT application, every tenth point is plotted (please note change in time scale bar). Thin dashed line indicates zero current level.

(C) Representative current passed by a cell expressing ΔKCNKØ E28C, T115C channels as in (C). Oocyte was perfused with 0.5 mM DTNB for 330 s (solid bar), then with 5 mM DTT for 1000 s (dashed bar), followed by a second application of 0.5 mM DTNB for 750 s (solid bar). Every third point plotted, zero current level at thin dashed line.

(D) The effect of DTT and DTNB on ΔKCNKØ channels and variants with single or double cysteine substitutions. While cells expressing ΔKCNKØ E28C, T115C channels were sensitive, neither DTT nor DTNB altered the function of ΔKCNKØ channels (inset: representative cell perfused with 5 mM DTT and then 0.5 mM DNTB in 5 mM potassium solution). DTT and DTNB also did not alter the current passed by cells expressing ΔKCNKØ channels with the single mutations E28C, T115C, or T114C, the double mutations E28C, A112C; E28C, P113C; E28C, T114C; or E28C, F116C. Measurements on groups of 4–8 cells as in (B), mean ± SEM; currents were assessed before and 3–5 min into perfusion with either 5 mM DTT (black bars) or 0.5 mM DNTB (gray bars). Cells expressing both ΔKCNKØ E28C and ΔKCNKØ T115C subunits (E28C + T115C) were also insensitive to both reagents.

Previously, we demonstrated that KCNKØ channel activity directly reflects the frequency and duration of visits to C_{long} (Zilberberg et al., 2000). Here, we report that external zinc blocks the channel after it leaves the open burst state to enter C_{long} and that C_{long} is limited in duration by bath potassium, suppressed by the external pore blocker TEA, sensitive to mutation, and modified by charge-altering covalent modifications near the extracellular mouth of the pore. These functional attributes are shared by C-type inactivation of Shaker channels. Moreover, mutation of homologous positions in KCNKØ and Shaker allows site-specific crosslinking to produce channels whose operation is determined by reducing and oxidizing agents. That changes in the external KCNKØ pore correspond directly to channel state suggests a gate resides in the outer KCNKØ pore that is similar to the C-type inactivation gate in VGK channels.

State-Dependent Block in the External Pore

Zinc blocks KCNKØ channels via H29 after the channels exit the O_{burst} state (Figures 1–3, Table 1). While observations of C_{Zn} were too rare to determine the conformation

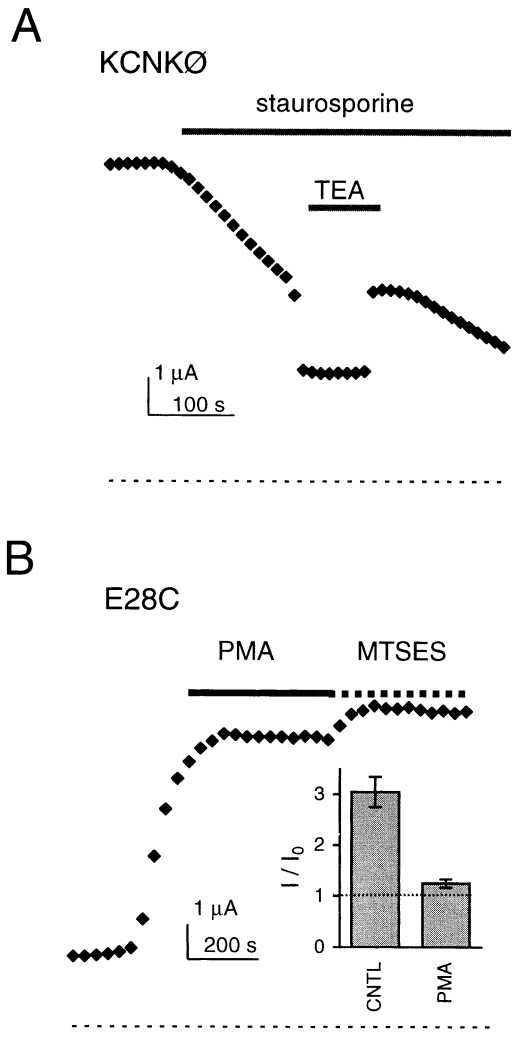

Figure 8. Regulated Activity and the External Pore

(A) Inhibition by external TEA impedes staurosporine-induced deactivation. Current passed by a cell expressing KCNKØ in control bath solution (5 mM potassium) and then staurosporine (2 μM) in the absence of TEA for 3 min followed by staurosporine with 95 mM TEA (isotonic exchange for sodium) for 100 s, before returning to staurosporine without TEA. Holding voltage was −80 mV and test pulses to 25 mV lasted 200 ms with a 10 s interpulse interval. Zero current level is indicated.

(B) MTSES (5 mM) has little effect if ΔKCNKØ E28C channels are first activated by 50 nM PMA (5 mM potassium solution). Protocol as in (A), every third point plotted. Inset: change in ΔKCNKØ E28C currents 4 min after application of 5 mM MTSES if untreated (CNTL) or activated by (PMA), mean ± SEM, n = 6 cells.

that zinc inhibits, we favor the simple idea that zinc blocks during C_{long} (rather than some other non-O_{burst} state) for the following reasons. KCNKØ channels activated by PMA are blocked by zinc slowly (Figure 1) and these channels leave O_{burst} to enter C_{long} only rarely (Zilberberg et al., 2000). Further, zinc inhibition rates correlate inversely with O_{burst} duration (Figure 2), indicating that channels in the open state are blocked infrequently. Moreover, zinc had no significant effect on unitary conductance or dwell times in the intraburst open or closed states (Table 1). Indeed, four manipulations that increased O_{burst} duration, including mutation (Figure 2E), raised external potassium (Figure 4), addition of external TEA (Figure 5), and chemical modification (Figure 6), all decreased the duration and frequency of C_{long} and, simultaneously, slowed the rate of zinc blockade (Figures 1E, 2E, 6E, and Results). KCNKØ channels are expected to form as homodimers, first, because channel subunits in this superfamily each carry two P-domains (Ketchum et al., 1995; Goldstein et al., 1996) and, second, because this stoichiometry is supported by study of proton blockade of a mammalian homolog, Kcnk3 (Lopes et al., 2001). We expect, therefore, that KCNKØ channels will carry two H29 residues, one on each subunit. Furthermore, we suspect that each channel has two zinc binding sites that are noninteracting and that zinc occupancy of one site is sufficient to inhibit. The rationale for these conjectures is as follows. As zinc levels increase, mean dwell time in C_{Zn} increases (Table 1); this is consistent with two binding sites where zinc on one site can block. Similarly, unblock is slower with increased zinc concentration (Figure 1D, legend), another expectation for multiple sites that function independently. A Hill coefficient for zinc inhibition of ~1 (Figure 1B) supports noninteraction of blocking sites. Further support for the notion that inhibition can proceed via zinc interaction with a single H29 site is that homologous residues in the structure of KcsA are not in proximity to one another (Figure 7A; Doyle et al., 1998) and that crosslinking just one of the four E418C-V451C pairs flanking a single P loop in Shaker channels appears sufficient to block (Larsson and Elinder, 2000); whether crosslinking a single E28C-T115C pair in KCNKØ is sufficient to inhibit is not yet known (Figure 7D).

C_{long} and C-Type Inactivation

VGK channels open an internal pore gate in response to depolarization and subsequently undergo C-type inactivation due to changes in the external pore; deactivation follows repolarization and entails reclosure of the internal gate (Baukrowitz and Yellen, 1996; Liu et al., 1997; Yellen, 1998; del Camino et al., 2000). KCNKØ channels do not alter their activity with voltage steps nor do they inactivate. Nonetheless, VGK channel C-type inactivation and KCNKØ opening and closing show notable similarities. First, C-type inactivation occurs at both positive and negative voltages so long as the activation gates are opened (Baukrowitz and Yellen, 1995, 1996; Miller and Aldrich, 1996), behavior comparable to the voltage-independent gating of KCNKØ (Zilberberg et al., 2000; Ilan and Goldstein, 2001). Further, C-type inactivation is inhibited by external permeant ions (Lopez et al., 1993; Baukrowitz and Yellen, 1995; Ogielska and Aldrich, 1999) just as single ΔKCNKØ channels reside in C_{long} 2- to 3-fold less frequently when external sodium is replaced by potassium, producing an ~5-fold increase in O_{burst} duration (Table 2).

Moreover, pore blockade by TEA slows VGK channel C-type inactivation (Grissmer and Cahalan, 1989; Choi et al., 1991), just as it increases O_{burst} duration of KCNKØ channels ~4-fold by suppressing entry into C_{long} (Table 2) and impedes staurosporine-induced deactivation (Figure 8A). That external potassium and TEA stabilize the open burst state (Table 2) and zinc does not inhibit

bursting channels (Figure 2E) appears to explain why both agents antagonize zinc inhibition (Figure 1E and Results).

In addition, position 449 in Shaker (and the homologous site in Kv1.4) has significant influence over C-type inactivation rate (Pardo et al., 1992; Lopez et al., 1993) and the presence of a cysteine at the site yields channels that bind external cadmium rapidly when in the C-type-inactivated state, stabilizing the conformation (Yellen et al., 1994; Liu et al., 1996). Similarly, mutation of the analogous position in KCNKØ (S112Y) yields channels that are more stable in C_{long} and show more rapid zinc blockade via H29 compared to wild-type (Table 2, Figure 2E). Unlike Shaker, a tyrosine at this site in KCNKØ does not produce a large increase in TEA affinity nor does a cysteine yield enhanced equilibrium blockade by cadmium (not shown); this may reflect the presence of four equivalent residues in Shaker whereas KCNKØ is expected to be 2-fold symmetric.

Just as interaction of zinc with KCNKØ via H29 is dependent on state, so the homologous residue in Shaker (A419) changes its local environment during C-type inactivation, as assessed by voltage clamp fluorometry (Loots and Isacoff, 2000). Further, like Shaker residues E418 and G452 (Larsson and Elinder, 2000), KCNKØ residues E28 and T115 appear to be in close proximity based on their ability to crosslink when altered to cysteine (Figure 7D). Discrepancies here include that Shaker 418 and 452 crosslink to stabilize an open state whereas KCNKØ 28 and 115 link to stabilize a closed state, and that Shaker 418 and 451 crosslink to stabilize a closed state while the homologous sites in KCNKØ (28 and 114) do not react. Of note, two other VGK channels, Kv1.3 (Bowlby et al., 1997; Fadool et al., 1997) and I_{Kr} in guinea pig ventricular myocytes (Heath and Terrar, 2000), appear to modulate C-type inactivation in a kinase-dependent fashion akin to the regulated entry of KCNKØ into C_{long} (Zilberberg et al., 2000).

KCNKØ and CNG Channels

Cyclic nucleotide-gated (CNG) channels are voltage independent, cation nonselective channels activated by intracellular binding of cyclic nucleotides. Similar in topology to VGK channels (with 1P/6TM subunits), CNG channels appear to employ an external activation gate as we posit for KCNKØ. Thus, conformational changes in the external CNG pore vestibule were demonstrated in association with cyclic-nucleotide-induced changes in channel activity (Liu and Siegelbaum, 2000). Moreover, at the internal site where VGK channels have a gate (Yellen, 1998; del Camino et al., 2000), CNG channels have only a restriction that gets smaller when the channels close, but does not restrict flux of small permeant ions (Craven and Zagotta, 2001; Flynn and Zagotta, 2001). In this work, the internal portion of the KCNKØ pore was not probed; however, the strong correlation of external pore function and activity suggests that, as for CNG channels, internal pore changes will not primarily determine KCNKØ gating.

Do Other 2-P-Domain Channels Open and Close Like KCNKØ?

It appears that similar but distinct gating mechanisms are at work in other KCNK channels. Like KCNKØ, KCNK2 also shows an increase in single channel Po (due to suppression of a long-closed state) when potassium is exchanged for rubidium (Bockenhauer et al., 2001) and macroscopic KCNK2 currents increase when external NMDG is replaced by potassium (Fink et al., 1996). However, KCNK2 channels are most notable for their capacity to undergo regulated and reversible interconversion between open rectifier phenotype (like KCNKØ) and voltage-dependent behavior by an unknown mechanism (Bockenhauer et al., 2001). KCNK3 channels also show increased outward current with elevated external potassium levels; however, in that case, a significant cause is potassium suppression of pore blockade by external proton (Lopes et al., 2000, 2001). Finally, the 2P/8TM outwardly rectifying potassium channel of *Saccharomyces cerevisiae*, TOK1, changes activity due to entry into a long-lasting closed state whose stability is altered by external potassium, the site analogous to Shaker 449, the viral peptide toxin K1, and pore mutations (Ketchum et al., 1995; Loukin et al., 1997; Vergani et al., 1998; Ahmed et al., 1999; Sesti et al., 2001). These findings suggest that KCNK2, KCNK3, and TOK1 also employ external gates; whether they are primary determinants of channel activity, as suggested for KCNKØ, remains to be ascertained.

Experimental Procedures

Molecular Biology

KCNKØ was cloned and cRNA synthesized using T7 polymerase and the mMESSAGE mMACHINE™ kit (Ambion) as described (Goldstein et al., 1996, 1999). Site-directed mutagenesis was performed with a QuikChange™ kit (Stratagene) and changes verified by DNA sequencing. Deletion mutants have been described previously (Zilberberg et al., 2000).

Electrophysiology

Xenopus laveis oocytes were isolated and injected with 23–46 nl containing 0.2–5 ng cRNA. Whole-cell currents were measured 1–4 days after injection by two-electrode voltage clamp (Warner Instruments Corp., Hamden, CT). Data were filtered at 0.5 kHz and sampled at 2 kHz. The patch-clamp technique was used to record single channels in on-cell patches 2–4 days after cRNA injection using an EPC-9 amplifier (HEKA elektronik, Germany) and data stored on videocassette. For analysis, records were sampled at and filtered as indicated using ACQUIRE (Bruxton Corporation, Inc., Seattle, WA) or Clampex software (Axon Instruments, Foster City, CA). Kinetic analyses were performed on patches judged to contain only one channel. Closed and open duration were determined using a half-amplitude threshold detected technique (Colquhoun and Sigworth, 1995) implemented using TAC software (Bruxton). Dwell-time distributions were plotted on a logarithmic time axis and a square-root vertical axis to best discern event populations (Sigworth and Sine, 1987). Dwell-time histograms were fitted using TacFit (Bruxton) to sums of exponential probability density functions using the maximum likelihood method with compensation to correct for missed events (Colquhoun and Sigworth, 1995).

Bath solution for two-electrode voltage clamp experiments contained (in mM): 0-98 KCl, 98-0 NaCl, 1 $MgCl_2$, 0.3 $CaCl_2$, 5 HEPES, pH 7.5 with NaOH. For patch-clamp, pipette and bath solutions contained (in mM): 140 KCl, 2 $MgCl_2$, 5 EGTA, 5 HEPES, pH 7.4 with KOH; this is close to a symmetrical potassium condition (Wang et al., 1996). Phorbol-12-myristate-13-acetate (PMA) and staurosporine were purchased from CALBIOCHEM (La Jolla, CA). For cysteine modifications, sodium (2-sulfonatoethyl) methanethiosulfonate (MTSES) was purchased from Toronto Research Chemicals (North York, Ontario, Canada) and dissolved in bath solution before each experiment. 5,5-dithio-bis(2-nitrobenzoic acid) (DTNB) (Sigma, St. Louis, MO) was dissolved daily in the recording solution. Stock

solution (1 M) of $CuSO_4$ and dry phenanthroline (Sigma, St. Louis, MO) were mixed daily in bath solution to prepare Cu/phenanthroline (4/200 μM) solution. All experiments were conducted at room temperature.

At zinc concentrations higher than 5 μM, macroscopic relaxation was well fitted by a single exponent decay function. However, at lower zinc levels, using two exponentials improved the fit (consistent with a multistep inhibition process). The slow time constant (120 ± 15 s, mean ± SEM, n = 10 cell, 5 mM potassium) had a much lower amplitude (~10%), so only the fast time constant was reported in the experiment reported here with 1 and 5 μM zinc (Figure 1D).

Acknowledgments

This work was supported by grants from the NIH to S.A.N.G., and the Human Frontier Science Program to N.Z. We are very grateful to E. Moczydlowski for help with the manuscript and F. Sesti and D. Goldstein for advice during the course of these studies.

Received March 26, 2001; revised September 18, 2001.

References

Ahmed, A., Sesti, F., Ilan, N., Shih, T.M., Sturley, S.L., and Goldstein, S.A.N. (1999). A molecular target for viral killer toxin: TOK1 potassium channels. Cell *99*, 283–291.

Backx, P.H., and Marban, E. (1993). Background potassium current active during the plateau of the action potential in guinea pig ventricular myocytes. Circ. Res. *72*, 890–900.

Baker, M., Bostock, H., Grafe, P., and Martius, P. (1987). Function and distribution of three types of rectifying channel in rat spinal root myelinated axons. J. Physiol. *383*, 45–67.

Baukrowitz, T., and Yellen, G. (1995). Modulation of K+ current by frequency and external [K+]: A tale of two inactivation mechanisms. Neuron *15*, 951–960.

Baukrowitz, T., and Yellen, G. (1996). Use-dependent blockers and exit rate of the last ion from the multi-ion pore of a K+ channel. Science *271*, 653–656.

Bockenhauer, D., Zilberberg, N., and Goldstein, S.A.N. (2001). KCNK2: reversible conversion of a hippocampal potassium leak into a voltage-dependent channel. Nat. Neurosci. *4*, 486–491.

Bowlby, M.R., Fadool, D.A., Holmes, T.C., and Levitan, I.B. (1997). Modulation of the Kv1.3 potassium channel by receptor tyrosine kinases. J. Gen. Physiol. *110*, 601–610.

Boyle, W.A., and Nerbonne, J.M. (1992). Two functionally distinct 4-aminopyridine-sensitive outward K+ currents in rat atrial myocytes. J. Gen. Physiol. *100*, 1041–1067.

Buckler, K.J., Williams, B.A., and Honore, E. (2000). An oxygen-, acid- and anaesthetic-sensitive TASK-like background potassium channel in rat arterial chemoreceptor cells. J. Physiol. (Lond.) *525*, 135–142.

Choi, K.L., Aldrich, R.W., and Yellen, G. (1991). Tetraethylammonium blockade distinguishes two inactivation mechanisms in voltage-activated K+ channels. Proc. Natl. Acad. Sci. USA *88*, 5092–5095.

Colquhoun, D., and Sigworth, F.J. (1995). Fitting and statistical analysis of single-channel records. In Single-Channel Recording, B. Sakmann and E. Neher, eds. (New York: Plenum Press), pp. 483–588.

Craven, K.B., and Zagotta, W.N. (2001). Conformational changes in the pore of rod cyclic nucleotide-gated channels revealed by state-dependent block. Biophys. J. *80*, 631a.

Czirjak, G., Fischer, T., Spat, A., Lesage, F., and Enyedi, P. (2000). TASK (TWIK-related acid-sensitive K+ channel) is expressed in glomerulosa cells of rat adrenal cortex and inhibited by angiotensin II. Mol. Endocrinol. *14*, 863–874.

del Camino, D., Holmgren, M., Liu, Y., and Yellen, G. (2000). Blocker protection in the pore of a voltage-gated K+ channel and its structural implications. Nature *403*, 321–325.

Demo, S.D., and Yellen, G. (1991). The inactivation gate of the Shaker K+ channel behaves like an open-channel blocker. Neuron *7*, 743–753.

Doyle, D.A., Morais Cabral, J., Pfuetzner, R.A., Kuo, A., Gulbis, J.M., Cohen, S.L., Chait, B.T., and MacKinnon, R. (1998). The structure of the potassium channel: molecular basis of K+ conduction and selectivity. Science *280*, 69–77.

Fadool, D.A., Holmes, T.C., Berman, K., Dagan, D., and Levitan, I.B. (1997). Tyrosine phosphorylation modulates current amplitude and kinetics of a neuronal voltage-gated potassium channel. J. Neurophysiol. *78*, 1563–1573.

Fink, M., Duprat, F., Lesage, F., Reyes, R., Romey, G., Heurteaux, C., and Lazdunski, M. (1996). Cloning, functional expression and brain localization of a novel unconventional outward rectifier K+ channel. EMBO J. *15*, 6854–6862.

Flynn, G.E., and Zagotta, W.N. (2001). Conformational changes in s6 coupled to the opening of cyclic nucleotide-gated channels. Neuron *30*, 689–698.

Goldman, D.E. (1943). Potential, impedance, and rectification in membranes. J. Gen. Physiol. *27*, 37–60.

Goldstein, S.A.N., Price, L.A., Rosenthal, D.N., and Pausch, M.H. (1996). ORK1, a potassium-selective leak channel with two pore domains cloned from Drosophila melanogaster by expression in Saccharomyces cerevisiae. Proc. Natl. Acad. Sci. USA *93*, 13256–13261.

Goldstein, S.A.N., Price, L.A., Rosenthal, D.N., and Pausch, M.H. (1999). Sequence correction for: ORK1, a potassium-selective leak channel with two pore domains cloned from Drosophila melanogaster. Proc. Natl. Acad. Sci. USA *96*, 318.

Goldstein, S.A.N., Bockenhauer, D., O'Kelly, I., and Zilberberg, N. (2001). Potassium leak channels and the KCNK family of two-P-domain subunits. Nat. Rev. Neurosci. *2*, 175–184.

Grissmer, S., and Cahalan, M. (1989). TEA prevents inactivation while blocking open K+ channels in human T lymphocytes. Biophys. J. *55*, 203–206.

Heath, B.M., and Terrar, D.A. (2000). Protein kinase C enhances the rapidly activating delayed rectifier potassium current, IKr, through a reduction in C-type inactivation in guinea-pig ventricular myocytes. J. Physiol. (Lond.) *522*, 391–402.

Hille, B. (1973). Potassium channels in myelinated nerve. Selective permeability to small cations. J. Gen. Physiol. *61*, 669–686.

Hille, B. (1975). Ionic selectivity of Na and K channels of nerve membranes. Membranes *3*, 255–323.

Hodgkin, A.L., Huxley, A.F., and Katz, B. (1952). Measurements of current-voltage relations in the membrane of the giant axon of Loigo. J. Physiol. *116*, 424–448.

Hoshi, T., Zagotta, W.N., and Aldrich, R.W. (1990). Biophysical and molecular mechanisms of Shaker potassium channel inactivation. Science *250*, 533–538.

Hoshi, T., Zagotta, W.N., and Aldrich, R.W. (1991). Two types of inactivation in Shaker K+ channels: effects of alterations in the carboxy-terminal region. Neuron *7*, 547–556.

Ilan, N., and Goldstein, S.A.N. (2001). KCNK0: single, cloned potassium leak channels are multi-ion pores. Biophys. J. *80*, 241–254.

Jones, S.W. (1989). On the resting potential of isolated frog sympathetic neurons. Neuron *3*, 153–161.

Ketchum, K.A., Joiner, W.J., Sellers, A.J., Kaczmarek, L.K., and Goldstein, S.A.N. (1995). A new family of outwardly-rectifying potassium channel proteins with two pore domains in tandem. Nature *376*, 690–695.

Kiss, L., and Korn, S.J. (1998). Modulation of C-type inactivation by K+ at the potassium channel selectivity filter. Biophys. J. *74*, 1840–1849.

Koh, D.S., Jonas, P., Brau, M.E., and Vogel, W. (1992). A TEA-insensitive flickering potassium channel active around the resting potential in myelinated nerve. J. Membr. Biol. *130*, 149–162.

Larsson, H.P., and Elinder, F. (2000). A conserved glutamate is important for slow inactivation in K+ channels. Neuron *27*, 573–583.

Liu, J., and Siegelbaum, S.A. (2000). Change of pore helix conformational state upon opening of cyclic nucleotide-gated channels. Neuron *28*, 899–909.

Liu, Y., Jurman, M.E., and Yellen, G. (1996). Dynamic rearrangement of the outer mouth of a K+ channel during gating. Neuron *16*, 859–867.

Liu, Y., Holmgren, M., Jurman, M.E., and Yellen, G. (1997). Gated access to the pore of a voltage-dependent K+ channel. Neuron *19*, 175–184.

Loots, E., and Isacoff, E.Y. (1998). Protein rearrangements underlying slow inactivation of the Shaker K+ channel. J. Gen. Physiol. *112*, 377–389.

Loots, E., and Isacoff, E.Y. (2000). Molecular coupling of S4 to a K+ channel's slow inactivation gate. J. Gen. Physiol. *116*, 623–635.

Lopes, C.M.B., Gallagher, P.G., Buck, M.E., Butler, M.H., and Goldstein, S.A.N. (2000). Proton block and voltage-gating are potassium-dependent in the cardiac leak channel Kcnk3. J. Biol. Chem. *275*, 16969–16978.

Lopes, C.M.B., Zilberberg, N., and Goldstein, S.A.N. (2001). Block of Kcnk3 by protons: evidence that 2-P-domain potassium channel subunits function as homodimers. J. Biol. Chem. *276*, 24449–24452.

Lopez, B.J., Hoshi, T., Heinemann, S.H., and Aldrich, R.W. (1993). Effects of external cations and mutations in the pore region on C-type inactivation of Shaker potassium channels. Receptors Channels *1*, 61–71.

Loukin, S.H., Vaillant, B., Zhou, X.L., Spalding, E.P., Kung, C., and Saimi, Y. (1997). Random mutagenesis reveals a region important for gating of the yeast K+ channel Ykc1. EMBO J. *16*, 4817–4825.

Millar, J.A., Barratt, L., Southan, A.P., Page, K.M., Fyffe, R.E., Robertson, B., and Mathie, A. (2000). A functional role for the two-pore domain potassium channel TASK-1 in cerebellar granule neurons. Proc. Natl. Acad. Sci. USA *97*, 3614–3618.

Miller, A.G., and Aldrich, R.W. (1996). Conversion of a delayed rectifier K+ channel to a voltage-gated inward rectifier K+ channel by three amino acid substitutions. Neuron *16*, 853–858.

Ogielska, E.M., and Aldrich, R.W. (1999). Functional consequences of a decreased potassium affinity in a potassium channel pore. Ion interactions and C-type inactivation. J. Gen. Physiol. *113*, 347–358.

Ortega-Saenz, P., Pardal, R., Castellano, A., and Lopez-Barneo, J. (2000). Collapse of conductance is prevented by a glutamate residue conserved in voltage-dependent K+ channels. J. Gen. Physiol. *116*, 181–190.

Pardo, L.A., Heinemann, S.H., Terlau, H., Ludewig, U., Lorra, C., Pongs, O., and Stuhmer, W. (1992). Extracellular K+ specifically modulates a rat brain K+ channel. Proc. Natl. Acad. Sci. USA *89*, 2466–2470.

Rettig, J., Heinemann, S.H., Wunder, F., Lorra, C., Parcej, D.N., Dolly, J.O., and Pongs, O. (1994). Inactivation properties of voltage-gated K+ channels altered by presence of beta-subunit. Nature *369*, 289–294.

Schmidt, H., and Stampfli, R. (1966). The effect of tetraethylammonium chloride on single Ranvier's nodes. Pflugers Arch. Gesamte Physiol. Menschen Tiere *287*, 311–325.

Sesti, F., Shih, T., Nikoleva, N., and Goldstein, S.A.N. (2001). The basis for immunity to killer toxin: channel block. Biophys. J. *80*, 446a.

Sigworth, F.J., and Sine, S.M. (1987). Data transformations for improved display and fitting of single-channel dwell time histograms. Biophys. J. *52*, 1047–1054.

Sirois, J.E., Lei, Q., Talley, E.M., Lynch, C., 3rd, and Bayliss, D.A. (2000). The TASK-1 two-pore domain K+ channel is a molecular substrate for neuronal effects of inhalation anesthetics. J. Neurosci. *20*, 6347–6354.

Talley, E.M., Lei, Q.B., Sirois, J.E., and Bayliss, D.A. (2000). TASK-1, a two-pore domain K+ channel, is modulated by multiple neurotransmitters in motoneurons. Neuron *25*, 399–410.

Vergani, P., Hamilton, D., Jarvis, S., and Blatt, M.R. (1998). Mutations in the pore regions of the yeast K+ channel YKC1 affect gating by extracellular K+. EMBO J. *17*, 7190–7198.

Wang, K.-W., Tai, K.-K., and Goldstein, S.A.N. (1996). MinK residues line a potassium channel pore. Neuron *16*, 571–577.

Wu, J.V., Rubinstein, C.T., and Shrager, P. (1993). Single channel characterization of multiple types of potassium channels in demyelinated Xenopus axons. J. Neurosci. *13*, 5153–5163.

Yellen, G. (1998). The moving parts of voltage-gated ion channels. Q. Rev. Biophys. *31*, 239–295.

Yellen, G., Sodickson, D., Chen, T.Y., and Jurman, M.E. (1994). An engineered cysteine in the external mouth of a K+ channel allows inactivation to be modulated by metal binding. Biophys. J. *66*, 1068–1075.

Yue, D.T., and Marban, E. (1988). A novel cardiac potassium channel that is active and conductive at depolarized potentials. Pfluegers Archives *413*, 127–133.

Zagotta, W.N., Hoshi, T., and Aldrich, R.W. (1990). Restoration of inactivation in mutants of Shaker potassium channels by a peptide derived from ShB. Science *250*, 568–571.

Zhou, M., Morais-Cabral, J.H., Mann, S., and MacKinnon, R. (2001). Potassium channel receptor site for the inactivation gate and quaternary amine inhibitors. Nature *411*, 657–661.

Zilberberg, N., Ilan, N., Gonzalez-Colaso, R., and Goldstein, S.A.N. (2000). Opening and closing of KCNK0 potassium leak channels is tightly-regulated. J. Gen. Physiol. *116*, 721–734.